Proceedings of the 9th U.S. National and 10th Canadian Conference on Earthquake Engineering
Compte Rendu de la 9ième Conférence Nationale Américaine et
10ième Conférence Canadienne de Génie Parasismique
July 25-29, 2010, Toronto, Ontario, Canada • Paper No 669

ANALYTICAL FRAGILITY CURVES FOR SEISMICALLY AND NON-SEISMICALLY DESIGNED MULTI-SPAN CONTINUOUS CONCRETE GIRDER BRIDGES IN MODERATE SEISMIC ZONES

K. Ramanathan[1], R. DesRoches[2] and J. E. Padgett[3]

ABSTRACT

Multi-span continuous concrete girder bridges are one of the most common bridge types in the central and south eastern United States. Proper understanding of their seismic response and quantitative and qualitative assessment of their seismic risk has gained prime focus in the earthquake engineering community due to the increased awareness of the seismic hazard in the central and southeastern US. Seismic fragility curves for these highway bridges are essential for risk assessment of highway transportation networks exposed to seismic hazards. This study focuses on developing and comparing fragility curves for seismically and non-seismically designed bridges pertinent to this region, using 3-D analytical models and nonlinear time-history analyses. Component and system fragility curves are obtained and are compared for the case of non-seismically and seismically designed bridges.

Introduction

Fragility curves, which are conditional probability statements that give the likelihood that the structure will meet or exceed a specified level of damage for a given ground motion intensity measure, have found widespread use in probabilistic seismic risk assessment of highway bridges. The conditioning parameter is typically a single intensity measure like peak ground acceleration (PGA) or spectral acceleration at the geometric mean of longitudinal and transverse periods. Fragility curves could be developed based on expert opinion, empirical data from past earthquakes (Basoz and Kiremidjian 1999, Shinozuka et al. 2003), and analytical methods (Nielson and DesRoches 2007, Mackie and Stojadinovic 2001, Jernigan and Hwang 2002, Mander and Basoz 1999). The current fragility curves used for seismic risk assessment of bridges are typically based on simplified analyses or empirical data from recent earthquakes. Since earthquake damage data are very scarce in the central and south eastern United States (CSUS), analytical method remains the only feasible approach to obtain fragility curves.

[1] Graduate Research Assistant, School of Civil & Environmental Engineering, Georgia Institute of Technology, Atlanta, GA 30332
[2] Professor & Associate Chair, School of Civil & Environmental Engineering, Georgia Institute of Technology, Atlanta, GA 30332
[3] Assistant Professor, Dept.of Civil &Environmental Engineering, Rice University, Houston, TX 77005

In 1990, bridges in the CSUS began incorporating seismic details. Some of the changes included the component design forces, design of columns and foundation, and treatment of liquefaction and liquefaction induced ground movement (Kawashima 2000). A detailed review of bridges in the national bridge inventory (NBI) built after 1990 in the CSUS region shows that multi-span continuous (MSC) concrete girder bridges account for approximately 25% of the bridges in the region. The present study focuses on developing fragility curves for seismically (S) and non-seismically (NS) designed MSC concrete girder bridges in CSUS. Choi (2004) examined over 150 bridge plans from this region and details regarding these bridges can be found in Nielson and DesRoches (2007). A review of the evolution in seismic design practices in the region reveals that the predominant difference between S-MSC and NS-MSC concrete bridges is associated with the detailing aspects in the columns. It is well known that transverse reinforcement has a major impact on the shear resistance, and ductility capacity of bridges. Several bridge columns experienced flexural shear failure at mid-height due to premature termination of longitudinal reinforcement primarily and insufficient spacing of transverse reinforcement, in a few cases during the 1995 Hyogo-ken nanbu earthquake (Kawashima 2000). Bridge piers designed in the CSUS after 1990 have greater splice lengths and reduced transverse reinforcement spacing. Modern seismically designed columns have higher transverse reinforcement ratios in the longitudinal and transverse directions, as a consequence of reduced spacing, when compared to the respective values in columns designed prior to 1990. Flexure thereby becomes the dominant behavior in seismically designed columns whereas shear often controls in non-seismically designed columns.

Prior to 1990, bridge columns in the CSUS typically had transverse reinforcement which consisted of #13 bars at a spacing of 305 mm on center. Whereas, in case of the seismically designed bridges, the spacing of the #13 stirrups is as close as 76 mm on center. In either case, multi column bents often consists of a rectangular reinforced concrete bent beam supported by 914 mm diameter circular columns. The effect of closely spaced transverse reinforcement is incorporated in the confined concrete material model which is discussed in subsequent sections.

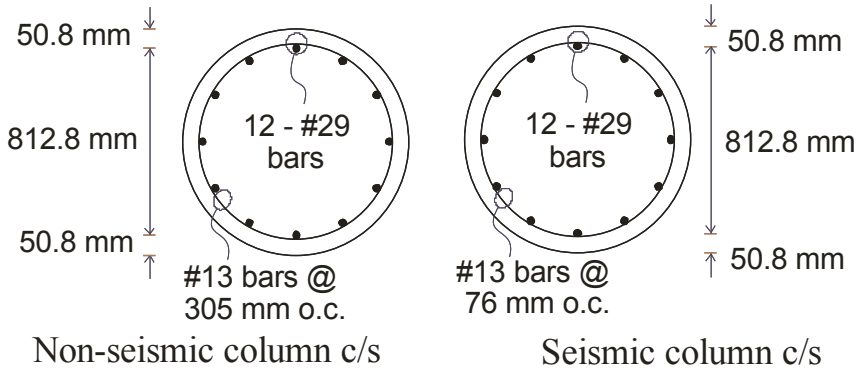

Figure 1. Typical seismic and non-seismic column cross-sections in CSUS.

While previous studies (Nielson and DesRoches 2007, Hwang et al. 2000) have evaluated the seismic response and fragility of various bridge classes common to the CSUS, there is little research that explores the differences in performance of typical CSUS bridges built with and without seismic detailing. This paper provides a first step by investigating the influence of

seismic detailing of MSC concrete bridges on the seismic performance, as well as the failure probability through the development and comparison of fragility curves.

Analytical Modeling of MSC Concrete Girder Bridges

Detailed 3-D models are generated for the bridges incorporating both geometrical and material non-linearities using the finite element platform OpenSEES (McKenna and Fenves 2005). The superstructure is modeled using elastic beam-column elements with mass lumped along the centerline. This is typical as the composite slab and girder generally behaves linearly. Pounding between the decks is considered using the contact element approach developed by Muthukumar and DesRoches (2006). The bearings and abutments are modeled using non-linear translational springs, accounting for the contribution of the elastomeric pads in addition to the steel dowels in the bearing elements. In case of the abutments, the model considers the contribution of both soil and the piles in the passive (compression) direction but considers the contribution of the piles alone in the active (tension) direction.

The columns are modeled using non-linear beam column elements with fiber defined cross sections. The non-linear hysteretic behavior of these columns is captured using a distributed plasticity element. Fiber defined cross sections enable specifying different properties for cover concrete and confined concrete. As mentioned previously, the difference between the modeling of the seismically and non-seismically designed bridges lies in the concrete model for the confined concrete. The effect of the closely spaced transverse reinforcement in the case of the seismically designed bridge columns is accounted for by using the confined concrete model developed by Mander et al. (1988). Fig. 2 shows the stress strain curve for confined concrete in the case of the S-MSC and the NS-MSC concrete bridge columns. In case of the S-MSC concrete bridge columns, the confined compressive strength, f_{con} is approximately 33% larger than f'_c and the ultimate strain, ε_{cu} is approximately 0.05. Whereas, in the case of the NS-MSC concrete bridge columns, f_{con} is approximately 7.1% larger than f'_c and the ultimate strain, ε_{cu} is only about 0.012. Other column details such as lap splices in plastic hinge regions are not considered explicitly in the current study's column models. The rectangular cross-section bent beams are also modeled using non-linear beam column elements, similar to the columns. Further details of the base bridge models can be found in Nielson and DesRoches (2007).

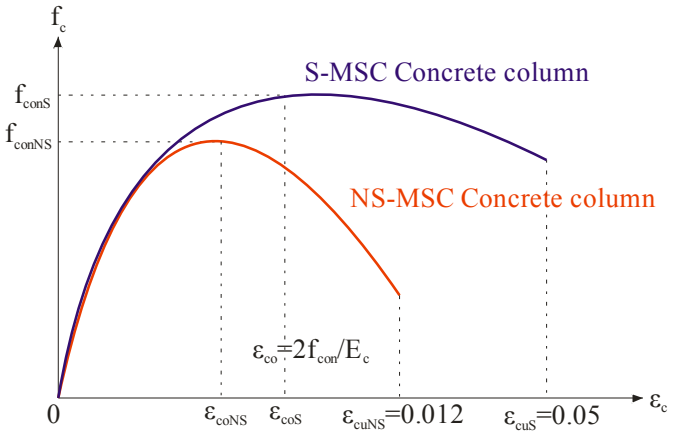

Figure 2. Confined Concrete model for S-MSC and NS-MSC concrete girder bridges.

Bridge Characteristics and Comparison of Seismic Response

The typical layout of a MSC Concrete girder bridge that is used in this study to compare the response of S-MSC and NS-MSC concrete bridges is shown in Fig. 3.

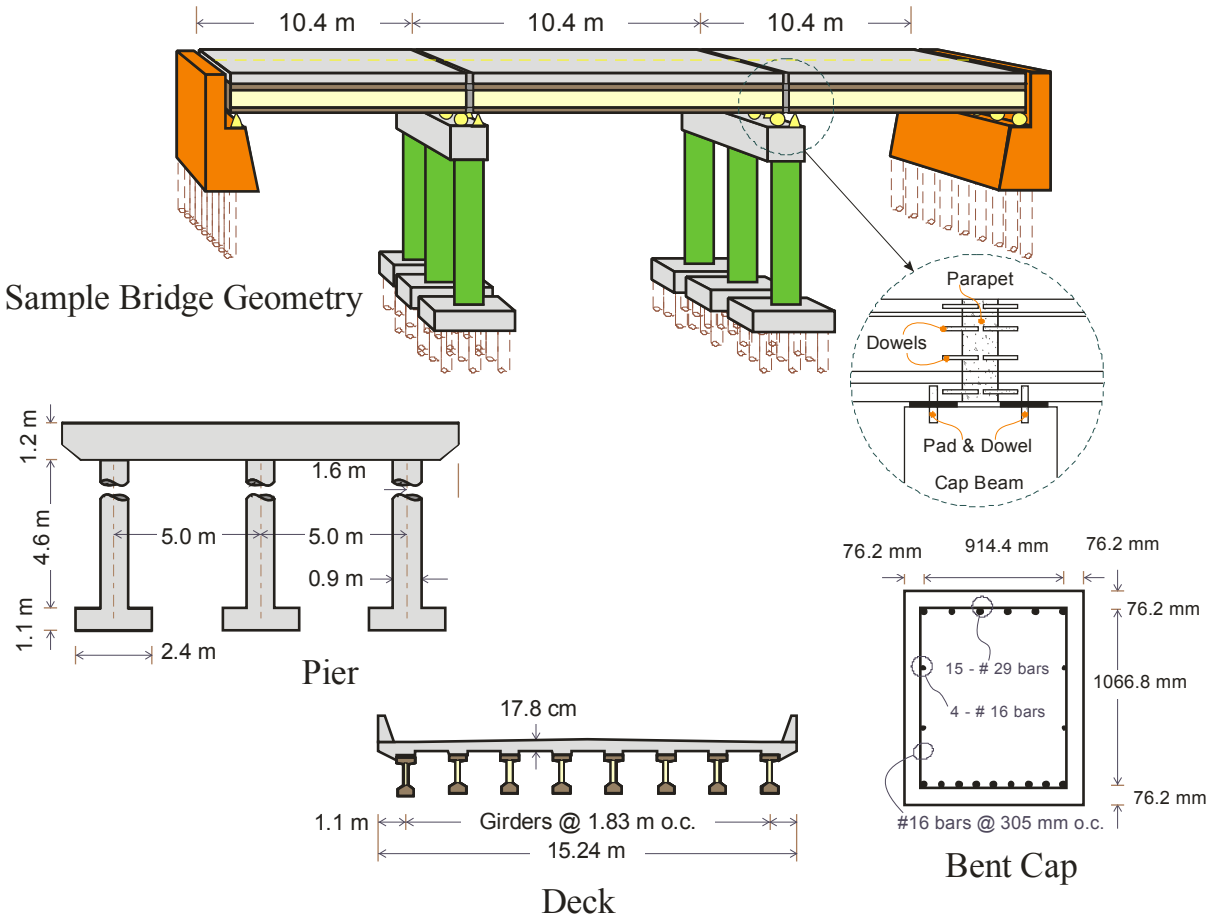

Figure 3. Typical layout of S-MSC and NS-MSC Concrete girder bridge.

The bridge fundamental mode is in the longitudinal direction with a period of 0.38 sec and the second mode is a transverse mode with a period of 0.29 sec. The bridges are subjected to the 1995 Kobe earthquake ground motion of 60 sec duration and peak ground acceleration (PGA) of 1.28g and 0.92g in longitudinal and transverse directions respectively, to illustrate the differences in seismic response. A common way of measuring the column demands is in terms of curvature ductility, μ, defined as the ratio of curvature that causes the first yielding of the outermost reinforcing bar and the maximum curvature in the column due to the seismic loading. From Fig. 4(a), it can be seen that the μ for S-MSC concrete bridge is about 3% greater than μ for NS-MSC concrete bridge. The abutments respond in both active and passive actions in the longitudinal direction as is illustrated in Fig. 4(b). In this case, it can be seen that the active action is dominant in case of both the bridges and the response is about 9% higher in case of the seismically designed bridge. The similar behavior can be seen in case of the elastomeric expansion bearing which is about 11% higher in S-MSC concrete bridges, from the force

deformation response shown in Fig. 4(c). It must be noted that these types of bearings might undergo large deformations that might result in bearings walking out from under the girders and thereby causing unseating. Also the deck displacements in case of the seismically designed bridges are about 20% higher as seen in Fig. 4(d).

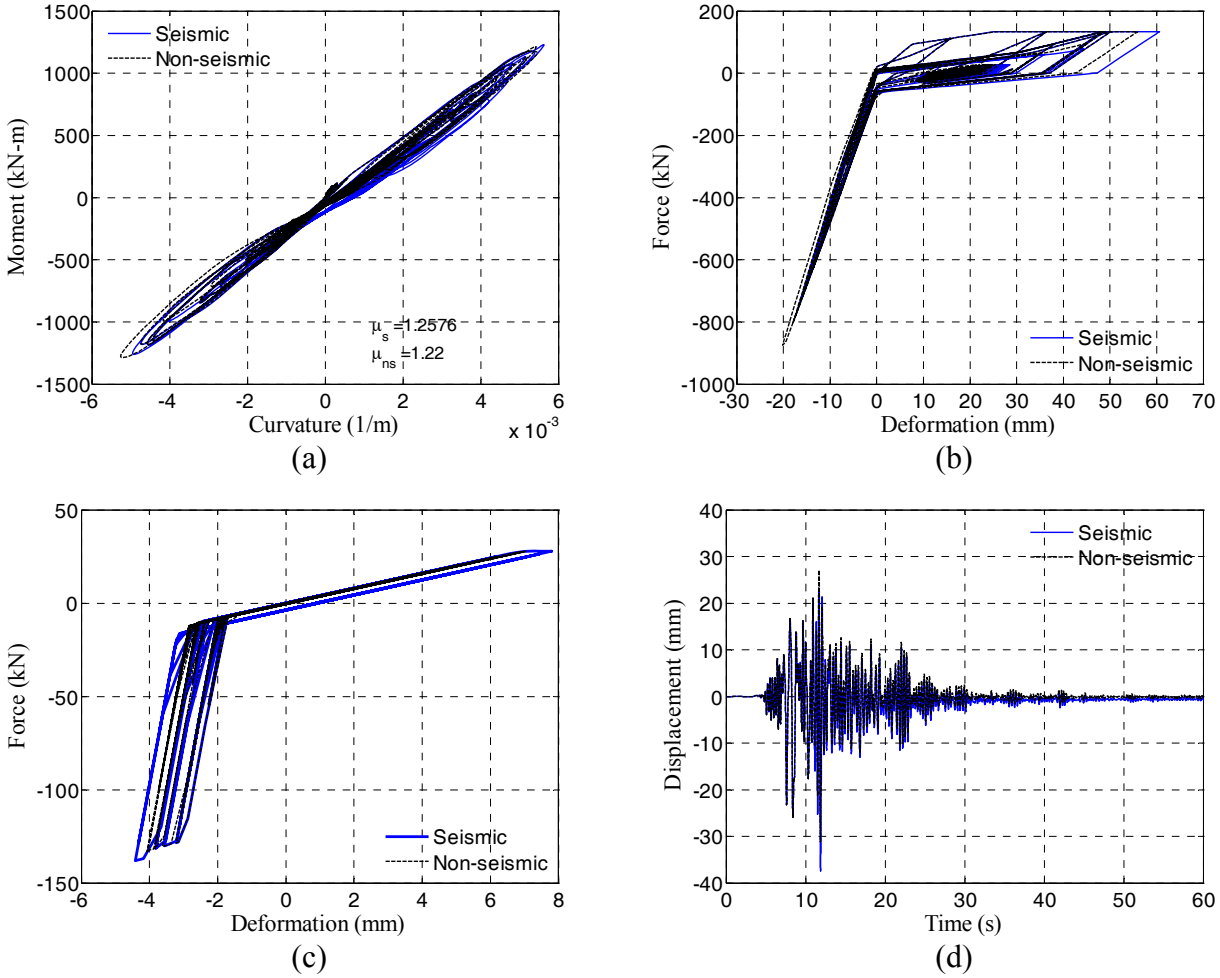

Figure 4. Comparison of responses in S-MSC and NS-MSC bridges for (a) columns, (b) abutments, (c) elastomeric expansion bearings and (d) deck displacements.

Ground Motion Suite

The analytical models are subjected to a suite of 48 ground motions developed by Rix and Fernandez-Leon (2004) characteristic to Memphis, TN. The 48 ground motions were selected such that there is a well balanced cross-section of PGA and spectral acceleration, S_a values. Each of the synthetic ground motion was used to generate two orthogonal components following the procedure outlined by Baker and Cornell (2006). The geometric mean of the PGA values of the orthogonal components varies between 0.03g and 0.74g and the geometric mean of the S_a at the fundamental periods in the longitudinal and transverse directions, $S_{a\text{-}gm}$ varies between 0.06g and 1.45g.

Probabilistic Seismic Demand Models and Fragility Curve Methodology

Fragility curves in this study are based on full 3-dimensional nonlinear time history analyses to estimate the seismic demand placed on the bridges. A fragility analysis simply assesses the probability that the seismic demand (D) placed on the structure exceeds the capacity (C) conditioned on a chosen intensity measure (IM) representative of the seismic loading. D and C are assumed to follow a lognormal distribution and the probability of reaching or exceeding a specific damage state for a particular component can be estimated using the standard normal cumulative distribution function, defined as,

$$P[D > C/IM] = \Phi\left(\frac{ln(S_d / S_c)}{\sqrt{\beta_{d/IM}{}^2 + \beta_c{}^2}}\right) \tag{1}$$

where, S_d is the median estimate of the demand as a function of IM, S_c is the median estimate of the capacity, $\beta_{d/IM}$ is the dispersion or logarithmic standard deviation of the demand conditioned on the IM, β_c is the dispersion of the capacity and $\Phi(\cdot)$ is the standard normal cumulative distribution function. Equation (1) can be evaluated by developing a probability distribution for demand conditioned on the IM, commonly known as probabilistic seismic demand model (PSDM), and convolving it with the capacity distribution. The set of analytical 3-D models is subjected to a suite of n ground motions and in each case the peak demand measures (e.g., column curvature ductility, bearing and abutment deformations) are recorded. The median demand, S_d can be expressed as a power function (Cornell et al. 2002):

$$S_d = a(IM)^b \tag{2}$$

where, a and b are regression coefficients. A linear regression of the demand – IM pairs in the transformed space determines the values of a and b. The dispersion of the demand conditioned on IM is given by,

$$\beta_{d/IM} = \sqrt{\frac{\sum_{i=1}^{n}\left(ln\, d_i - ln\, a(IM)^b\right)^2}{n-2}} \tag{3}$$

Geometric and material variabilities, such as concrete and steel strengths, component behaviors, deck gaps, loading direction, mass, damping, are considered in the model via probability distributions. Nominally identical yet statistically significant bridge samples are generated through Latin Hypercube Sampling. The representative geometries and parameter distributions are consistent with those posed by Nielson and DesRoches (2007) to facilitate comparison with the seismically designed bridge. The study deals with a broad class of bridges and hence PGA and $S_{a\text{-}gm}$ are the chosen intensity measures (Padgett et al. 2007). Fig.5 shows the demand plots for columns and fixed elastomeric bearings in the longitudinal direction as a function of PGA and $S_{a\text{-}gm}$ respectively.

The PSDMs for all of the bridge components of S-MSC and NS-MSC concrete bridges as a function of PGA is given in Table 1, where R^2 is the coefficient of determination indicating the accuracy of fit. There is a very minor difference in demand in S-MSC and NS-MSC concrete bridges. This is expected since the initial stiffness for both cases is identical, and the maximum compressive strength only shows in small difference between the seismically and non-seismically designed bridge columns. The critical effect of the non-seismically designed column is not necessarily an effect on the demand but rather a reduction in capacity. Hence, limit states are most critical when considering changes only in column detailing.

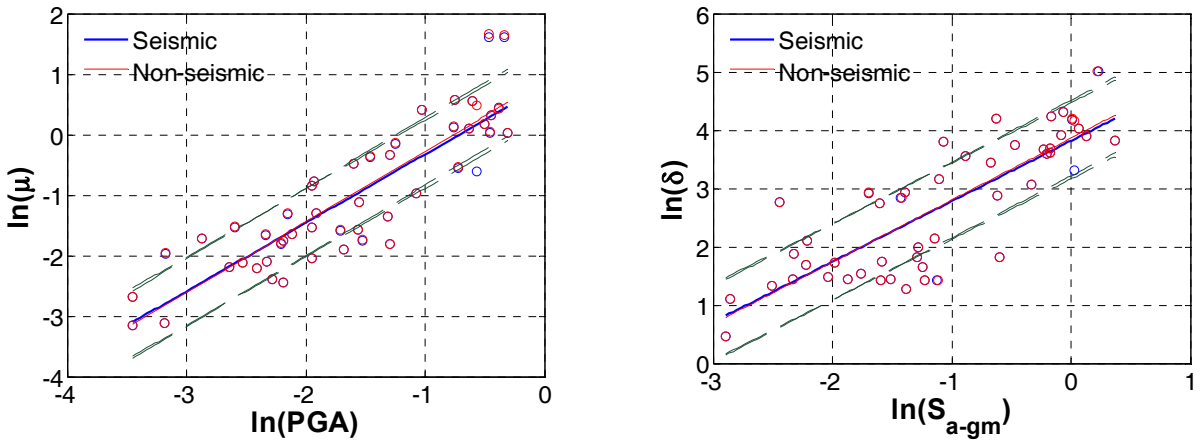

Figure 5. Comparison of PSDMs for (a) Column curvature ductility vs. PGA, (b) elastomeric fixed bearing deformation vs. $S_{a\text{-}gm}$ for S-MSC and NS-MSC concrete bridges.

Table 1. PSDM estimates for various components.

Component	Seismic				Non-seismic			
	a	***b***	$\beta_{d/PGA}$	R^2	***a***	***b***	$\beta_{d/PGA}$	R^2
Column	0.8	1.13	0.56	0.76	0.89	1.17	0.56	0.78
Elasto fixed bearing-longitudinal	4.23	0.98	0.73	0.59	4.34	1.01	0.73	0.61
Elasto fixed bearing-transverse	3.05	0.78	0.91	0.37	3.08	0.80	0.90	0.38
Elasto expan bearing-longitudinal	4.25	0.87	0.58	0.64	4.29	0.89	0.58	0.65
Elasto expan bearing-transverse	3.03	0.78	0.91	0.37	3.07	0.79	0.89	0.38
Abutment - passive	3.00	1.06	0.79	0.59	3.16	1.13	0.77	0.63
Abutment - active	2.58	0.50	0.81	0.24	2.60	0.51	0.80	0.25
Abutment - transverse	2.58	0.83	0.63	0.58	2.59	0.84	0.62	0.59

Component Limit States

The components considered in this study are columns, fixed and expansion elastomeric bearings and abutments (active and passive as well as transverse).The component limit states are also assumed to be lognormally distributed. The median, S_c and the dispersion, β_c values of the capacity limit states are obtained from experimental results and are then updated based on results from a survey conducted by Padgett and DesRoches (2007) using the theory of Bayesian updating. The study uses four damage states; slight, moderate, extensive and complete,

comparable to those found in HAZUS-MH (FEMA 2003). The table below summarizes limit states adopted for the various bridge components, while further details can be found in Nielson and DesRoches (2007). Additionally, the limit states for the columns in the seismically designed bridges are obtained from experimental studies in the PEER column structural performance database (Berry and Eberhard 2003).

Table 2. Bridge component limit states.

	Slight		Moderate		Extensive		Complete	
Component	S_c	β_c	S_c	β_c	S_c	β_c	S_c	β_c
Column (non seismic)	1.44	0.73	2.70	0.61	3.92	0.74	4.18	0.77
Column (seismic)	4.89	0.7	9.15	0.53	12.46	0.59	13.08	0.59
Elasto fixed bearing-long (mm)	28.9	0.60	104.2	0.55	136.1	0.59	186.6	0.65
Elasto fixed bearing-(trans) (mm)	28.8	0.79	90.9	0.68	142.2	0.73	195.0	0.66
Elasto expan bearing-(long) (mm)	28.9	0.60	104.2	0.55	136.1	0.59	186.6	0.65
Elasto expan bearing-(trans) (mm)	28.9	0.60	104.2	0.55	136.1	0.59	186.6	0.65
Abutment - passive (mm)	37.0	0.46	146.0	0.46	N/A	N/A	N/A	N/A
Abutment - active (mm)	9.8	0.70	37.9	0.90	77.2	0.85	N/A	N/A
Abutment - trans (mm)	9.8	0.70	37.9	0.90	77.2	0.85	N/A	N/A

Component and system fragility curves

Having estimated the demand and capacity parameters, the fragility curves for various bridge components can be obtained based on the closed form given in Equation (1). In order to estimate the bridge system level fragility, Nielson and DesRoches (2007) proposed the use of joint probabilistic seismic demand models (JPSDM). The JPSDM is developed by assessing the demands placed on each component (marginal distribution) through a regression analysis as in the case of PSDMs. The covariance matrix is assembled by estimating the correlation coefficients between the demands placed on the various components. A Monte Carlo simulation is then used to compare realizations of the demand (using the JPSDM defined by a conditional joint normal distribution in the transformed space) and statistically independent component capacities to calculate the probability of system failure. This procedure is repeated across a range of IM for each of the damage states. Regression analysis is used to estimate the lognormal parameters (median, λ and standard deviation or dispersion, ζ) which characterize the bridge system fragility. The fragility curves for the S-MSC and NS-MSC concrete bridges are shown in Fig. 6 and the median, λ and standard deviation or dispersion, ζ, values are given in Table 3.

Table 3. Median and dispersion values for fragility curves.

	Slight		Moderate		Extensive		Complete	
Intensity measure (IM)	λ	ζ	λ	ζ	λ	ζ	λ	ζ
PGA (g) S-MSC	0.16	0.983	0.794	0.936	1.210	0.899	1.762	0.880
$S_{a\text{-}gm}$ (g) S-MSC	0.28	0.893	1.279	0.889	1.919	0.849	2.759	0.811
PGA (g) NS-MSC	0.154	0.964	0.655	0.793	0.928	0.783	1.159	0.775
$S_{a\text{-}gm}$ (g) NS-MSC	0.272	0.860	1.073	0.765	1.494	0.749	1.876	0.726

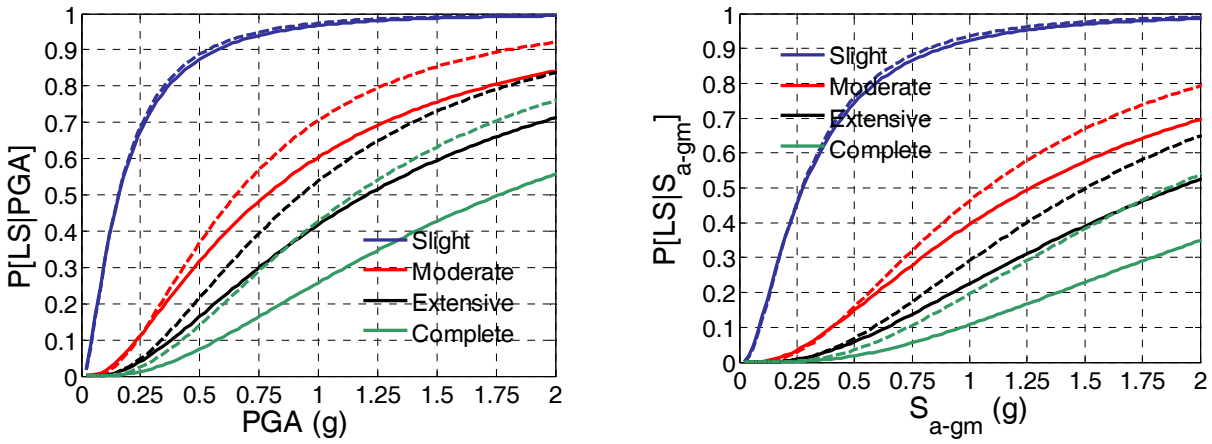

Figure 6. System fragility curves for seismically and non-seismically designed bridges. Dashed lines indicate non-seismic design while solid lines indicate seismic design.

From Fig. 6, we see that there is a minor difference in the curves at the slight damage state. This is because the transverse abutment response dominates the vulnerability at this damage state. Hence, a significant improvement is not seen due to seismic detailing of the columns which has little effect on the demand and more effect on the capacity. Furthermore, it is seen that the Elastomeric fixed bearings dominate the vulnerability in case of the moderate, extensive and complete damage states.

A simple technique to compare differences in the fragility curves is to evaluate the relative change in the median value of the fragility curves. A positive change indicates a less vulnerable structure while a negative change indicates a more vulnerable structure. The percent changes in median values for the system fragility curves of S-MSC and NS-MSC concrete bridges are 3.9%, 21.2%, 30.4% and 52% for slight, moderate, extensive and complete damage states respectively with PGA as the IM (2.9%, 19.2%, 28.5%, 47.1% with $S_{a\text{-}gm}$ as the IM) . It is evident that there is a considerable difference in the median values when seismic detailing is provided. The difference is well pronounced in the higher limit states as expected.

Conclusions

This paper presents an analytical method for the development of fragility curves of seismically and non-seismically designed MSC concrete girder bridges typical to the Central and Southeastern US. The curves are developed based on full non-linear time history analyses of 3-D analytical models subjected to a suite of ground motions for CSUS. The predominant difference in the two classes of bridges is the detailing in the column which involves increased transverse reinforcement ratio due to reduce spacing. The capacities or limit states for non-seismically designed bridges are consistent with those in Nielson and DesRoches (2007) to facilitate comparison, while those for the seismically designed bridges are obtained based on tests of seismic columns reported in the PEER column structural performance database. The fragility analysis considers the vulnerability of various bridge components like columns, elastomeric expansion and fixed bearings and abutments and combines them to achieve system level fragility curves.

Though the effect of seismic detailing of the concrete column does not yield a significant difference in the probabilistic seismic demand models for the two classes of bridges, the increase in capacity results in a bridge that is much less vulnerable to the extensive and complete levels of damage at the system level. This can be attributed to the fact that the columns are traditionally one of the most vulnerable components of the MSC concrete bridge class at the upper damage states. The fragility analysis reveals an increase in the median fragilities of the seismically designed bridges is as high as 52% considering PGA as an intensity measure (47% considering $S_{a\text{-}gm}$) for the complete damage state. There is a negligible impact at the slight damage state due to the dominance of the transverse abutment response which is not affected in the current study's assumption of seismic design detailing.

References

Baker, J. and Cornell, A. C., 2006. Which Spectral Acceleration Are You Using?, *Earthquake Spectra*, 22(2).

Basoz, N. and Kiremidjian, A. S., 1999. Development of empirical fragility curves for bridges, *Proceedings of the 5th US Conference on Lifeline Earthquake Engineering: Optimizing Post-Earthquake Lifeline System Reliability,* 693–702.

Berry, M. P. and Eberhard, M. O., 2004. *PEER structural performance database user's manual*, Pacific Earthquake Engineering Research Center University of California, Berkeley CA.

Choi, E., DesRoches, R., and Nielson, B., 2004. Seismic Fragility of Typical Bridges in Moderate Seismic Zones, *Engineering Structures*, 26(2), 187–199.

Cornell, A. C., Jalayer, F., Hamburger, R. O., and Foutch, D. A., 2002. Probabilistic basis for 2000 SAC Federal Emergency Management Agency steel moment frame guidelines, *Journal of Structural Engineering*, 128, 526-532.

Hwang, H., Jernigan, J. B., Lin, Y. W., 2000. Evaluation of seismic damage to Memphis bridges and highway systems, *Journal of Bridge Engineering*, 5(4), 322-330.

Kawashima, K., 2000. Seismic Design and Retrofit of Bridges, *Bulletin of the New Zealand National Society for Earthquake Engineering*, 33(3), 265-285.

Mackie, K and Stojadinovic, B., 2001. Probabilistic Seismic Demand Model for California Highway Bridges, *Journal of Bridge Engineering*, 6(6), 468-480.

Mander, J. B., and Basoz, N., 1999. Seismic fragility curve theory for highway bridges, *5th US Conference on Lifeline Earthquake Engineering,* Seattle, WA, USA, ASCE.

Mander, J. B., Priestley, M. J. N., and Park, R., 1988. Theoretical stress-strain model for confined concrete, *Journal of Structural Engineering*, 114(8), 1804-1826.

McKenna, F. and Fenves, G. L. 2005. Open System for Earthquake Engineering Simulation Pacific Earthquake Engineering Research Center, Version 1.6.2.

Muthukumar, S., 2003. A Contact Element Approach with Hysteresis Damping for the Analysis and Design of Pounding in Bridges, *Ph.D. Thesis*, Georgia Institute of Technology, Atlanta, GA.

Nielson, B. and DesRoches, R., 2007. Analytical Seismic Fragility Curves for Typical Bridges in the Central and Southeastern United States, *Earthquake Spectra*, 23(3), 615-633.

Nielson, B. and DesRoches, R., 2007. Seismic fragility methodology for highway bridges using a component level approach, *Earthquake Engineering and Structural Dynamics*, 36, 823-839.

Padgett, J. E., Nielson, B. G. and DesRoches, R., 2007. Selection of optimal intensity measures in probabilistic seismic demand models of highway bridge portfolios, *Earthquake Engineering and Structural Dynamics*, 37, 711-725.

Padgett, J. E. and DesRoches, R., 2007. Bridge Functionality Relationships for Improved Seismic Risk Assessment of Transportation Networks, *Earthquake Spectra*, 23(1), 115-130.

Shinozuka, M., Feng, M. Q., Kim, H., Uzawa, T. and Ueda, T., 2003. Statistical Analysis of Fragility Curves, *Report No. MCEER-03-0002,* MCEER.